PNAS RESEARCH ARTICLE | EVOLUTION

Evolutionary divergent kinetoplast genome structure and RNA editing patterns in the trypanosomatid *Vickermania*

Evgeny S. Gerasimov[a], Dmitry A. Afonin[a,1], Ingrid Škodová-Sveráková[b,c,d], Andreu Saura[b], Natália Trusina[c], Ondřej Gahura[d], Alexandra Zakharova[b,2], Anzhelika Butenko[b,d,e], Peter Baráth[f,g], Anton Horváth[c], Fred R. Opperdoes[h], David Pérez-Morga[i], Sara L. Zimmer[j], Julius Lukeš[d,e,3], and Vyacheslav Yurchenko[b,3]

Affiliations are included on p. 8.

Contributed by Julius Lukeš; received December 23, 2024; accepted March 5, 2025; reviewed by Laurie K. Read and Kenneth Stuart

The trypanosomatid flagellates possess in their single mitochondrion a highly complex kinetoplast (k)DNA, which is composed of interlocked circular molecules of two types. Dozens of maxicircles represent a classical mitochondrial genome, and thousands of minicircles encode guide (g)RNAs, which direct the processive and essential uridine insertion/deletion messenger RNA (mRNA) editing of maxicircle transcripts. While the details of kDNA structure and this type of RNA editing are well established, our knowledge mostly relies on a narrow foray of intensely studied human parasites of the genera *Leishmania* and *Trypanosoma*. Here, we analyzed kDNA, its expression, and RNA editing of two members of the poorly characterized genus *Vickermania* with very different cultivation histories. In both *Vickermania* species, the gRNA-containing heterogeneous large (HL)-circles are atypically large with multiple gRNAs each. Examination of *Vickermania spadyakhi* HL-circle loci revealed a massive redundancy of gRNAs relative to the editing needs. In comparison, the HL-circle repertoire of extensively cultivated *Vickermania ingenoplastis* is greatly reduced. It correlates with *V. ingenoplastis*-specific loss of productive editing of transcripts encoding subunits of respiratory chain complex I and corresponding lack of complex I activity. This loss in a parasite already lacking genes for subunits of complexes III and IV suggests an apparent requirement for its mitochondrial adenosine triphosphate (ATP) synthase to work in reverse to maintain membrane potential. In contrast, *V. spadyakhi* retains a functional complex I that allows ATP synthase to work in its standard direction.

Vickermania | RNA editing | kinetoplast DNA | trypanosomatids | ATP synthase

Significance

The study of trypanosomatid flagellates has continually broadened our knowledge of eukaryotic biology and highlighted the limits of our assumptions based on model organisms. The impacts of gains and losses of DNA units, such as extrachromosomal plasmids or pathogenicity islands, are relatively well-understood. However, across the tree of life, other instances of this process abound, with implications unexplored. In two closely related unicellular eukaryotes of the family Trypanosomatidae, we investigated the high and low complexity of a repertoire of guide RNA-containing molecules and their profound impact on the respiratory cycle in general and ATP synthase in particular.

The trypanosomatid flagellates have an array of unique features, but two particularly stand out. One is the mitochondrial, or kinetoplast (k)DNA, that is composed of relaxed circles forming a single colossal DNA network in the reticulated mitochondrion of these parasites (1). The other is uridine insertion/deletion (U-indel) RNA editing of the kDNA-derived protein-coding transcripts (2, 3). The reasons for the emergence of these features have been extensively debated but still remain speculative (4, 5). The massive expansion of mitochondrial DNA that has resulted in the largest organelle genomes currently known seems to have occurred prior to the separation of kinetoplastid flagellates (to which trypanosomatids belong) and the related diplonemids (6). The abundant presence of U-indel editing in the early-branching *Perkinsela* (7) implies that this process predates the emergence of the kDNA network in the derived trypanosomatids (8). Indeed, all members of this obligatory parasitic group have a single large kDNA catenane, typically composed of several thousand minicircles encoding an extensive repertoire of guide (g)RNAs directing the targeted insertion or removal of U-indels, and about a dozen identical protein-coding maxicircles analogous to other mitochondrial genomes (9). In the model species *Trypanosoma brucei*, transcripts of 12 out of 18 maxicircle-encoded protein-coding genes undergo U-indel editing to different extents. This complex and stepwise process proceeds in the 3′ to 5′ direction along an mRNA and, by inserting over 3,000 and deleting about 300 U residues across all edited transcripts, generates translatable products. U-indel editing requires the highly coordinated activity of up to hundreds of different guide (g)RNAs and several large complexes with a dynamic composition of over 70 proteins collectively (2). Unresolved are whether differential editing can result in more than one protein being generated from a single mRNA and the role editing plays in the regulation of trypanosomatid life cycles (10, 11). Due to the processive nature of U-indel editing and the presence of a substantial number of transient, alternative, and/or dead-end editing patterns, only a small fraction of mRNAs represents translatable products (12–14). Only the completely edited transcripts are furnished with long poly(A/U)-tails and subsequently bound by protein complexes that recruit ribosomes (15). While species-specific differences exist in

Author contributions: E.S.G., J.L., and V.Y. designed research; E.S.G., D.A.A., I.Š.-S., A.S., N.T., A.Z., P.B., and D.P.-M. performed research; E.S.G. and D.A.A. contributed new reagents/analytic tools; E.S.G., D.A.A., I.Š.-S., O.G., A.B., A.H., F.R.O., D.P.-M., S.L.Z., J.L., and V.Y. analyzed data; and E.S.G., S.Z., J.L., and V.Y. wrote the paper.

Reviewers: L.K.R., University at Buffalo; and K.S., Center for Infectious Disease Research.

The authors declare no competing interest.

[1]Present address: Fox Chase Cancer Center, Temple University Hospital, Philadelphia, PA 19111-2497.

[2]Present address: ChemRar High Tech Center, Khimki, Moscow oblast 141401, Russia.

[3]To whom correspondence may be addressed. Email: jula@paru.cas.cz or vyacheslav.yurchenko@osu.cz.

This article contains supporting information online at https://www.pnas.org/lookup/suppl/doi:10.1073/pnas.2426887122/-/DCSupplemental.

Published April 9, 2025.

efficiency and the degree of sequence identity needed for the binding of gRNAs to mRNA during editing, no major departure from the U-indel editing fundamentals have yet been observed among trypanosomatids (16, 17).

It is entirely possible, however, that trypanosomatids of the genus *Vickermania*, known for the unique presence of two flagella throughout most of their life cycle (18), may prove to harbor surprising departures from the canonical kDNA structure and U-indel editing paradigm known from *T. brucei* and other trypanosomatids. The early detected presence of large, loosely arranged circular kDNA molecules (HL-circles) in *V. ingenoplastis* (19) certainly pointed in that direction. Moreover, while in other trypanosomatid species, kDNA invariably assumes the shape of a densely packed disc attached to the basal body of the single flagellum in a cristate mitochondrion (20, 21), in *Vickermania* spp., the kDNA is teardrop-shaped and ensconced within a virtually acristate organelle (18, 22, 23). The analysis of the *Vickermania ingenoplastis* genome predicted an absence of the respiratory chain complexes III and IV (cIII and cIV), subunits of which are encoded in standard mitochondrial genomes (24, 25).

The genus *Vickermania* currently includes two species parasitizing flies: *V. ingenoplastis* isolated in the United States (26) was subjected to decades-long cultivation and *Vickermania spadyakhi* from Northern Russia (18) with very limited history in culture. Here, we demonstrate that gRNAs are transcribed from the HL-circles of both species, yet the productive editing of mitochondrial transcripts that ultimately results in an active nicotinamide-adenine dinucleotide (NADH) dehydrogenase, occurs only in *V. spadyakhi*. Additionally, our intraspecies comparison of encoded gRNAs and their products provides information on the selective loss of U-indel RNA editing in Trypanosomatidae and the intriguing connection between ATP synthase and mitochondrial architecture.

Results

The Entire Maxicircle Conserved Region (CR) Is Transcribed in Both *Vickermania* Species. Almost half-a-century ago, it was demonstrated that *V. ingenoplastis* lacks characteristic minicircles but, instead, possesses extremely large HL-circles along with typical maxicircles (19, 27). We initiated our study by confirming that the physical dimensions of the kDNA of the isolate available today after prolonged cultivation are similar to that reported in the early 1980s. We show the length and width of the spread kDNA network, periphery included, to be 8.1 ± 2 μm and 6.1 ± 2 μm (n = 11), respectively (*SI Appendix*, Fig. S1), similar to the earlier observations (19, 27). We also documented the presence of large circular molecules.

Next, we analyzed *Vickermania* kDNA organization by assembling the maxicircles focusing primarily on the CRs that harbor the rRNA and mRNA gene loci. Utilizing next-generation sequencing reads from both total DNA and kDNA libraries, we were subsequently able to obtain the entire 47,971 bp-long *V. ingenoplastis* maxicircle (GenBank PQ679924), of which a portion was determined previously (24). The repetitive nature of the *V. spadyakhi* maxicircle divergent region prevented its full assembly from short reads, so only the CR was assembled (GenBank PQ679925). The maxicircle CRs of both species have 28% GC-content, share 78% identity, and are near-identical in length (10,683 and 10,679 bp).

The ~11 kb *Vickermania* CRs are shorter than the typical ~16 kb trypanosomatid CRs (16), since the gene encoding CYb, the sole mitochondrial-encoded cIII subunit, along with those encoding COI, COII, and COIII subunits of cIV, have been lost, as is also true for plant-infecting trypanosomatids of the genus *Phytomonas* (28). Otherwise, the CR genes are syntenic with those of most trypanosomatids (Fig. 1). The genes for *ND1*, *ND2*, *ND4*, and *ND5* subunits of complex I (cI) and the gene encoding mitoribosomal protein RPS3 (*MURF5*) were identified, as were the G-rich cryptogenes *G3*, *G4*, *ND3*, *ND8*, *ND9*, and *RPS12*. The presence of cryptogenes *ND7*, *A6*, and *MURF2*, which contain much shorter blocks of G-rich sequences and require only limited editing to produce translatable mRNAs, was verified by BLASTn search using *Leptomonas pyrrhocoris* query sequences (29).

Combined maxicircle-derived reads from mRNA sequencing libraries of total and kinetoplast RNAs were used to compare the maxicircle expression profiles of *V. ingenoplastis* and *V. spadyakhi* after mapping reads, both those with and without U-indels, onto the respective maxicircle sequences (Fig. 1). The entire maxicircle CR of both species is transcribed, with variable read depths across the region of interest. Species-specific transcript abundance

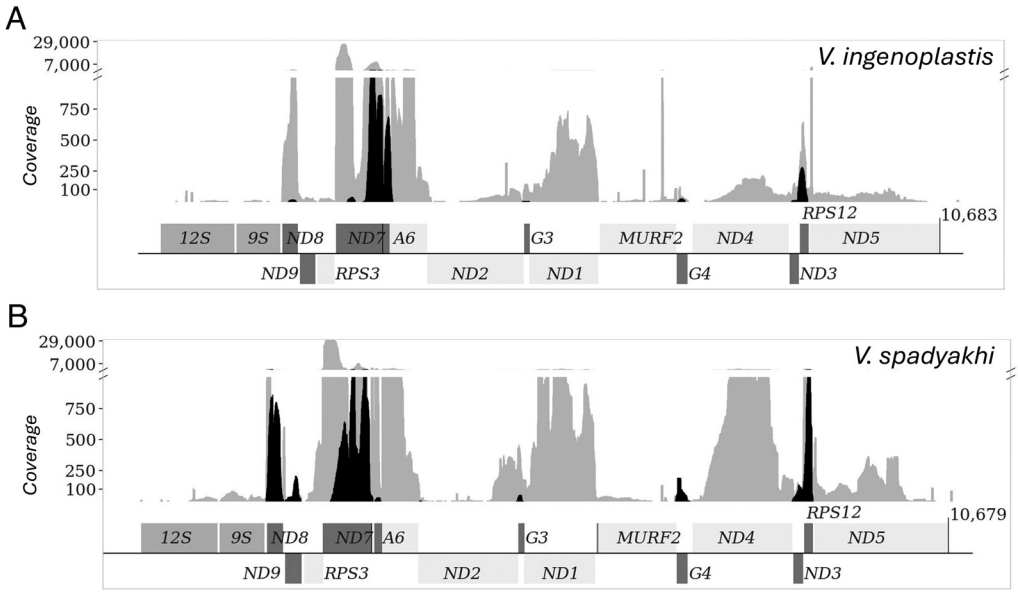

Fig. 1. Organization, transcription, and editing profiles of *V. ingenoplastis* (*A*) and *V. spadyakhi* (*B*) maxicircle CRs. *Bottom* panel of each profile depicts the annotation: medium gray, ribosomal RNAs; light gray, unedited genes; dark gray, edited cryptogenes. Cryptogenes *G3* and *G4* are also termed *CR3* and *CR4*, or *ND4L* and *ND6*, the latter being putative functional assignments of their protein products, primarily due to their hydrophobicity. Transcription and editing profiles are shown above. Gray, unedited reads' coverage; black, edited (10 or more edited sites) reads' coverage.

patterns failed to demonstrate coregulated abundance of functionally related genes. For example, transcription of some cI subunits is higher in *V. spadyakhi* (e.g., *ND1*, *ND4*, *ND5*, and *ND9*), yet comparable in both species for others (e.g., *ND2*, *ND7*, and *ND8*). Species-specific abundance patterns also emerge for edited reads (defined as those with 10 or more U-indels) (Fig. 1).

Translatable Edited mRNAs Are Species-Specific. Due to the stochastic and processive nature of the U-indel editing mechanism, the mitochondrial transcriptome contains pre-, partially-, fully-, and never-edited mRNAs (11). We generated full-length edited products for cryptogenes using T-Aligner that was designed to assemble edited reads into protein-coding sequences for each locus (12). The same read libraries mapped to maxicircle CRs (Fig. 1) were used as input for T-Aligner reconstruction. Given that all cryptogenes are expressed, some robustly, it was surprising that for *V. ingenoplastis*, we were able to reconstruct only fully edited mRNAs for *A6* that encodes a subunit of F_o ATP synthase, *RPS12* encoding a mitoribosomal protein, and *MURF2* with a short editing domain (*MURF2* encodes a protein of unassigned function). *V. ingenoplastis A6* appears to be present as two isoforms, one of which has a 54 nt-long truncation at its 5′ end due to an alternative editing pattern that changes the reading frame (*SI Appendix*, Fig. S2). The alternatively translated protein would initiate with a different 14 amino acids from a start codon internal to the start site typical of other trypanosomatids. No mature edited mRNAs could be reconstructed for any of the cI subunit cryptogenes (*ND3*, *ND7*, *ND8*, and *ND9*) or for two cryptogenes encoding proteins of unknown function (*G3* and *G4*) (Fig. 2). This is despite the fact that edited reads originating from each of these loci exist, albeit at lower abundances than in *V. spadyakhi*. In contrast, *V. spadyakhi* reconstructions resulted in mature edited mRNAs for full-length *A6*, *G3*, *G4*, *MURF2*, *ND3*, *ND7*, *ND8*, *ND9*, and *RPS12* cryptogenes. While only the standard length *A6* is reconstructed for this species, two slightly different isoforms each are reconstructed from alternative editing patterns in the *ND3* and *RPS12* reads. The editing pattern for the alternative RPS12 isoform results in a protein in which the last amino acid of the standard RPS12 is different and followed by an additional 12 amino acids. An alternative editing pattern for *T. brucei* RPS12 positioned seven codons upstream of the stop codon (13) also apparently results in a protein with a similarly sized C-terminal extension, albeit of different sequence. Therefore, longer and shorter RPS12 isoforms due to termini extensions may be widely tolerated.

Our inability to reconstruct most mature mRNAs of *V. ingenoplastis* cryptogenes could be due to lower number of edited reads as compared to *V. spadyakhi* (Fig. 1). However, patterns of major editing events in key cryptogenes strongly suggest that our findings are neither artifacts nor consequences of technical limitations. For *RPS12* that is productively edited in both species, the major editing patterns (as represented by the darkest dots on editing matrices in Fig. 2 *A* and *B*) are largely conserved between species, with *V. ingenoplastis* reads showing fewer editing events overall. Conversely, a reason why *V. ingenoplastis* mature *ND7* cannot be reconstructed is that nearly all editing occurs within a small domain at its 3′ terminus, in what appears to be a random pattern when compared with that of *V. spadyakhi* (Fig. 2 *C* and *D*). Single gRNAs are often sufficient to guide editing events in domains as short as that of *V. ingenoplastis ND7* (Fig. 2*D*). Given a lack of canonical pattern in this initial

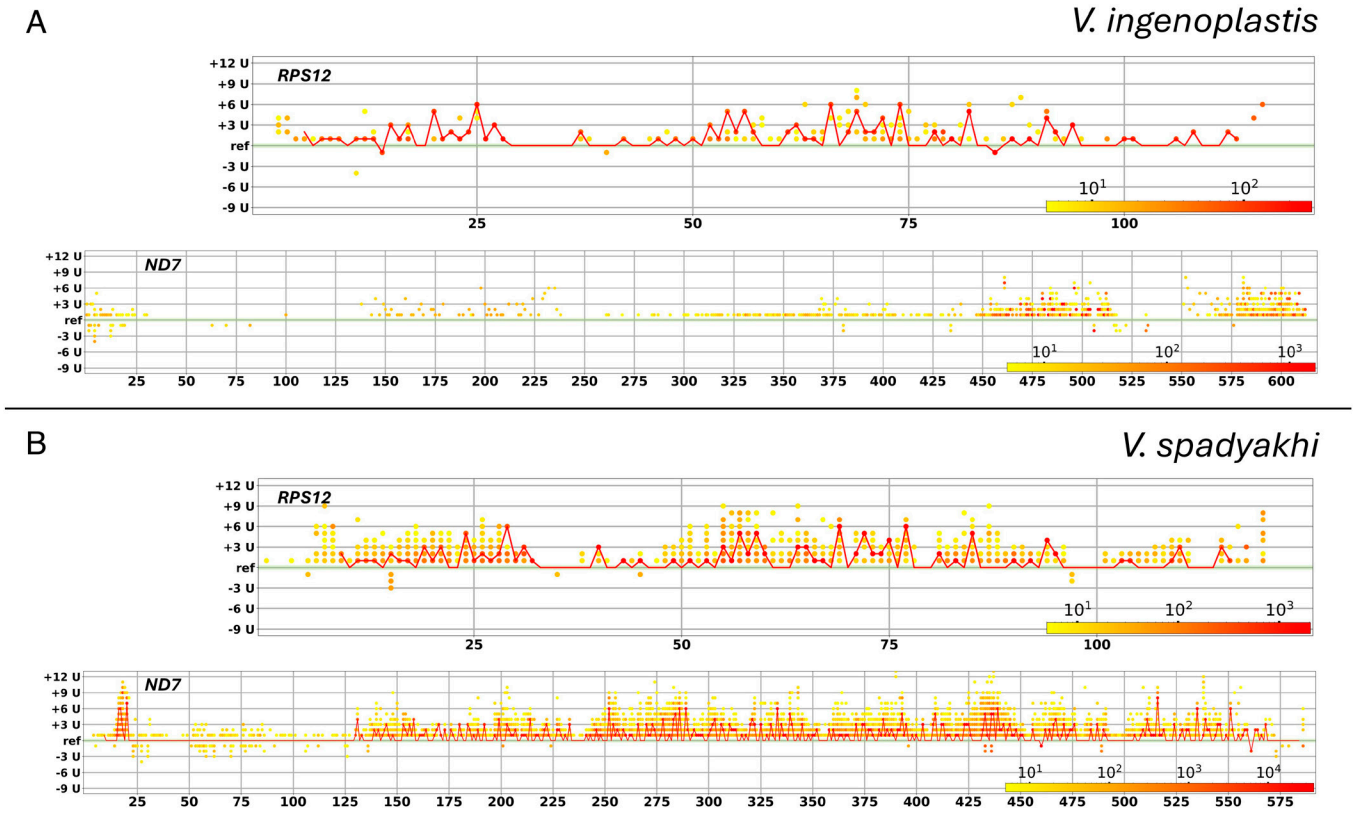

Fig. 2. T-Aligner editing plots for cryptogenes *RPS12* and *ND7* of *V. ingenoplastis* (*A*) and *V. spadyakhi* (*B*). The plot shows editing states for each cryptogene position as dots. The *X* axis denotes the position of A/G/C nucleotide in cryptogene reference. The *Y* axis denotes insertions (y > 0) and deletions (y < 0) of uridines from the cryptogene sequence, the reference number of Us corresponds to Y = 0 (green line at "ref" level). Dot color gradient reflects read support for the editing state (yellow for low support and red for high support, positions supported by two reads or less are not shown). Solid red line drawn across the editing states denotes the canonical editing pathway (except for *ND7* of *V. ingenoplastis*, because no canonical mRNA was reconstructed for it), which is the sequence of edits that generate a canonical open reading frame. The coordinates of *X* axis are DNA reference-based. The reference start coordinates for *V. ingenoplastis ND7* and *RPS12* are 2,474 and 8,762 bp, respectively; for *V. spadyakhi ND7* and *RPS12*, they are 3,396 and 9,762 bp, respectively.

editing domain, it would be difficult (if not impossible) for a successive guide RNA (gRNA) to bind this newly edited sequence, effectively shutting down any upstream editing. Therefore, the specific losses of editing in *V. ingenoplastis* are, most likely, an evolved outcome.

Species-Specific HL-Circle and gRNA Repertoires Are Consistent with Differences in Editing. *Vickermania* HL-circles, known only to be considerably larger than conventional minicircles (19, 27), have not yet been thoroughly characterized. We assembled and compared the HL-circle repertoires for *V. ingenoplastis* and *V. spadyakhi* to define their parameters. It is well established that conserved sequence block 3 (CSB3) and/or other specific motifs are typically found near the gRNA loci on kDNA minicircles. For example, a typical *Leishmania* minicircle gRNA locus occurs at a fixed distance from CSB3 and is upstream of a conserved adenine+thymine (AT)-rich motif (30). In assembled HL-circles, CSB3 was documented in multiple copies in cassettes, themselves present in polar pairs per circle (Fig. 3*A* and *SI Appendix*, Fig. S3). We also found an inverted repeat sequence (IRS), GTAATA-$(N)_n$-TATTAC, with a mean of five copies per HL-circle. The median distance between the repeat boundaries $(N)_n$ was calculated to be 30 bp. As this is a typical gRNA length, these IRSs may flank gRNA loci on HL-circles.

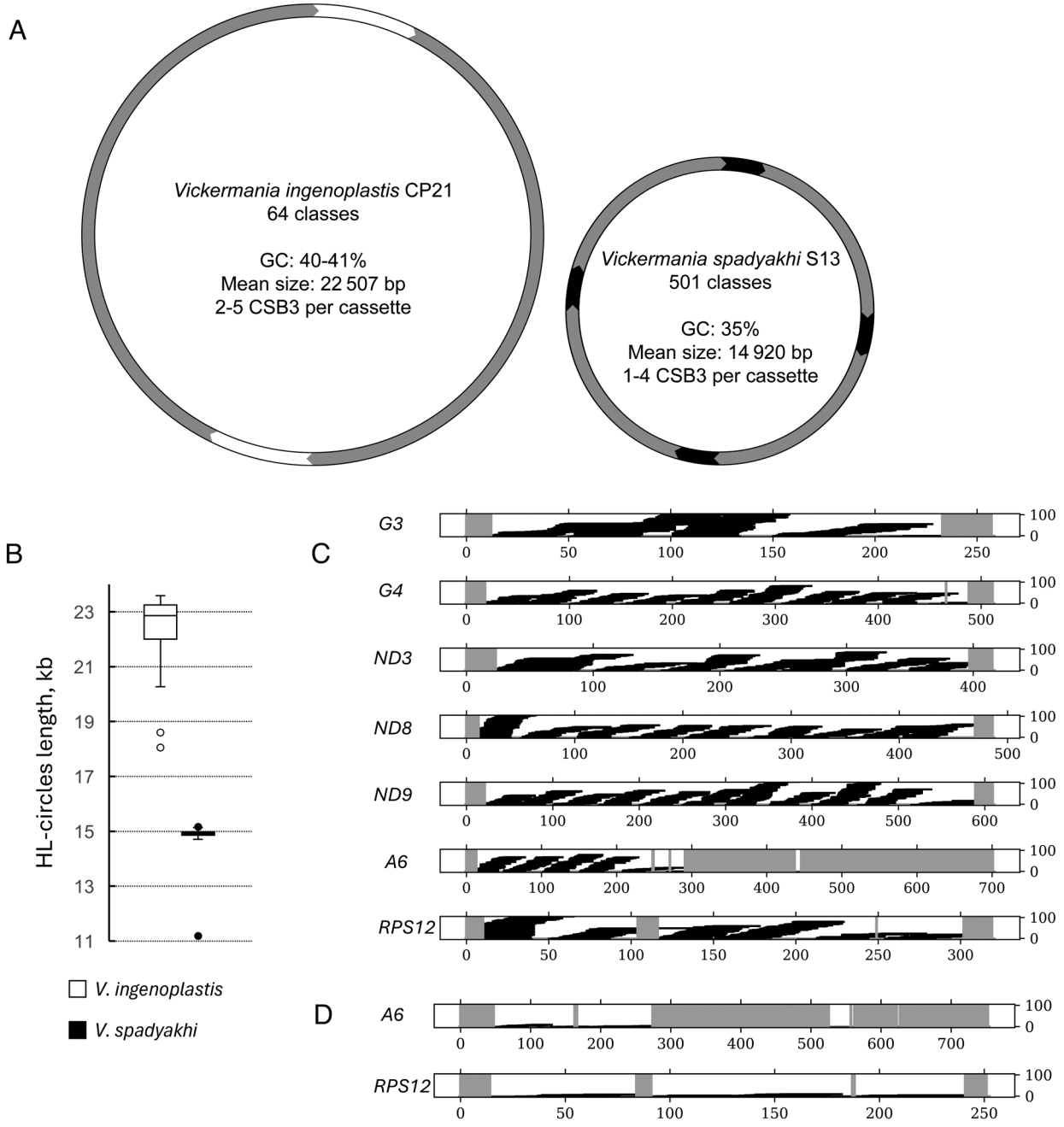

Fig. 3. HL-circles of *Vickermania spp*. (*A*) Size, repertoire, and near-universal arrangement of cassette motifs on *Vickermania spp.* HL-circles. Cassettes positioned at poles (depicted in white for *V. ingenoplastis* and black for *V. spadyakhi*) are regions containing one or more CSB3 20-mer motifs. (*B*) Size range of analyzed HL-circles. HL-circles larger or smaller than the 95% CI for population size are indicated with open (*V. ingenoplastis*) or solid (*V. spadyakhi*) dots. (*C* and *D*) Guide RNAs of *V. spadyakhi* (*C*) and *V. ingenoplastis* (*D*) positioned on their respective canonically edited mRNA. Regions not covered by any gRNAs are shown in light gray, gRNA alignments are depicted by stacked black lines. The *Y* axis depicts the number of independent gRNA loci identified by mRNA:HL-circle alignment analysis for each indicated cryptogene in the stack of overlapping gRNAs that are similarly positioned.

Other elements in HL-circles are species-specific. While HL-circles are significantly larger than minicircles in general, they are especially massive in *V. ingenoplastis* with a mean length of 22.5 kb, compared to 15 kb in *V. spadyakhi* (Fig. 3*B*). Additionally, the numbers of CSB3 repeats per cassette and cassettes per molecule vary by species (*SI Appendix*, Fig. S3*B*). Given their AT-richness and presence of the CSB3 motifs (Fig. 3*A*), HL-circles may have evolved from minicircles, although factors responsible for such an extensive divergence are unknown. Other conserved minicircle motifs, such as CSB1 and CSB2, and any protein-coding regions, are absent. Most potentially relevant to RNA editing, only 64 HL-circle classes were assembled for *V. ingenoplastis*, dwarfed by the 501 classes for *V. spadyakhi* (Dataset S1).

The larger *V. spadyakhi* HL-circle repertoire implies a larger set of gRNAs, which would be consistent with its more extensively edited transcriptome (Fig. 1). To computationally test this, we annotated all potential gRNA-coding loci by aligning each species' HL-circle repertoire with its reconstructed mature edited mRNAs using relaxed thresholds for alignment length, maximal number of G:U matches, and maximal number of mismatches (termed "raw" alignments). We subsequently intersected the mRNA hits on each HL-circle with positions of its IRSs. Hits located within the IRSs were deemed bona fide gRNA loci. There was an extremely low number of putative *V. ingenoplastis* gRNA loci (128 total) relative to species such as *T. brucei* with ~900 gRNA loci (17), and, as expected, to *V. spadyakhi*, which encodes 5,033 putative gRNAs (including cases of different, but partially overlapping, gRNAs originating from the same IRSs) (Table 1 and Dataset S1).

As an additional measure of the accuracy of the bona fide *Vickermania* spp. gRNA loci, we determined how gRNAs identified by this workflow correlate with those identified using a previously applied method that relies on rigorous thresholds for alignment length, maximal number of G:U matches, and maximal number of mismatches to eliminate false positives (16, 29). Not surprisingly, alignments intersecting with the IRSs and the IRSs themselves have similar median lengths, while raw alignments prior to filtering are considerably shorter (*SI Appendix*, Fig. S4). Shorter alignments were previously shown to often be false gRNA positives. Since the gRNA population sizes delineated by the IRS-guided and previous approaches were similar (*SI Appendix*, Fig. S4), we have more confidence in both of these methods of gRNA repertoire identification.

Table 1. HL-circles assembly and annotation

	V. ingenoplastis	*V. spadyakhi*
General stats:		
Total HL-circles	64	501
Total IRS	363	3,359
IRS per circle, median	5	5
Total HL-circles length	1,437,284	7,471,718
Average HL-circle size	22,458	14,914
Native mRNAs set:		
Raw alignments	1,659	86,845
intersects IRS	128	5,033
IRS covered by alignment	25%	79%
Total query length (mRNAs)	1,006	5,638
Cross-species mRNAs set:		
Raw alignments	10,233	13,600
intersects IRS	593	947
IRS covered by alignment	77%	79%
Total query length (mRNAs)	5,638	1,006

A minicircle-driven loss of editing of cI cryptogene transcripts was described for the UC strain of *Leishmania tarentolae* as a consequence of prolonged cultivation, during which cI became dispensable (31). Similarly, the highly reduced number of *V. ingenoplastis* gRNAs relative to those of *V. spadyakhi* is likely tied to the loss of productive editing of cI subunit-encoding cryptogenes in the former species. To confirm this, we aligned each species' IRS-flanked sequences and their edited mRNAs, revealing that 79% of *V. spadyakhi* IRS-internal sequences align to one of its edited mRNAs (Table 1). The identity of the remaining 21% of these sequences must then be either entirely nonfunctional, or else specify gRNAs that are not involved in editing of any of the identified canonical mRNAs. Since only *A6* and *RPS12* could be used for similar alignments in *V. ingenoplastis*, it is not surprising that only 25% of its already-low number of 363 total IRSs-flanked sequences mapped to these transcripts. We hypothesize that most of the 75% remaining *V. ingenoplastis* IRSs-flanked sequences (of note, they are not transcriptionally silent) encode cryptic gRNAs previously needed for editing of the transcripts encoding cI subunits, and *G3* and *G4* mRNAs.

To quantify the editing potential of these cryptic *V. ingenoplastis* gRNAs, we did a cross-species search with the complete set of *V. spadyakhi* mRNAs as queries against *V. ingenoplastis* IRSs-flanked sequences (Table 1). With the cross-species query, the percentage of aligned motifs increased to 77%, very close to the 79% documented for the *V. spadyakhi* IRSs-bound sequences identified in the same-species analysis. A reciprocal experiment with aligned *V. ingenoplastis* mRNAs identified the same 79% putative gRNAs of *V. spadyakhi*. This strongly suggests that the majority of *V. ingenoplastis* gRNA loci encode molecules utilizable in productive editing of *V. spadyakhi* mRNAs. To determine the likelihood of this cross-specific feature, we mapped the putative gRNAs of *V. ingenoplastis* onto *V. spadyakhi A6*, *G3*, *G4*, *ND3*, *ND8*, *ND9*, and *RPS12* edited mRNAs. The gRNA coverage reveals that these transcripts, productively edited in *V. spadyakhi*, could be covered by the set of *V. ingenoplastis* gRNAs with just a few gaps, presumably due to the interspecies sequence divergence and/or occasional gRNA loss during cultivation. However, the average coverage redundancy score for these alignments [the sum of lengths for all gRNAs aligning to the edited areas of each mRNA over the edited region length (32)] was 2.1, much lower than the score of 18 obtained when analyzing the coverage of the same mRNAs by *V. spadyakhi* gRNAs (Fig. 3*C*).

We next simulated HL-circle populations of 500 molecules, each having five gRNA loci for *A6*, *G3*, *G4*, *ND3*, *ND7*, *ND8*, *ND9*, and *RPS12* distributed randomly. Typically, only about 110 molecules out of the 500 set contains neither an *A6* nor *RPS12* gRNA and could thus be considered dispensable. However, the HL-circles repertoire of *V. ingenoplastis* consists of 64 classes, considerably less than 110. This means that some *A6* or *RPS12* gRNA loci-containing HL-circles are dispensable for survival, most likely due to the high gRNA redundancy of the recently isolated *V. spadyakhi* (Fig. 3*C*). This contrasts with the low redundancy in *V. ingenoplastis*, even across the presumably essential *A6* and *RPS12* transcripts (Fig. 3*D*). The relevance of this finding likely extends beyond *Vickermania*, as a lack of the cryptogene-specific partitioning of gRNAs among minicircles was also documented in *T. brucei* (17, 33).

Activity Assays Reveal the Outcomes of kDNA Gene Expression and Editing. It is clear that cIII and cIV of the electron transport chain (ETC) are absent in *Vickermania* spp. (25) (Fig. 1 and Dataset S2). However, a compelling question is whether the two examined species

differ in their possession of a functional cI-type NADH dehydrogenase, as we were unable to detect any of the kDNA-encoded canonically edited cI subunits in *V. ingenoplastis*, yet could readily reconstruct all of them in *V. spadyakhi*. Thus, at the gene expression level, only *V. spadyakhi* possesses all kDNA-encoded components of a functional cI. To biochemically address the functionality of *Vickermania* spp. cI, we analyzed their in-gel activity using *Phytomonas serpens* as a positive control (34). No activity was detected in either *Vickermania* spp. after 4 h (Fig. 4*A*, panel NDH 4 h), but after 24 h staining, distinct bands consistent with the cI size in *P. serpens* appeared in the *V. spadyakhi* lysate, but not in that of *V. ingenoplastis* (Fig. 4*A*, panel NDH 24 h). To further validate their identity, both stained bands of *V. spadyakhi* were excised from the gel and analyzed by mass spectrometry (Dataset S3). The identification of three peptides each of *V. spadyakhi* ND7 and ND8 proteins, conceptually translated in silico from the corresponding full-length reconstructed edited mRNAs (Fig. 4*B*), confirms the accuracy of the T-Aligner program in determining mature mRNAs of maxicircle-encoded genes. More importantly, however, it strongly indicates that cI is functional in this species. Correspondingly, the transcriptomic-based prediction of missing cI in *V. ingenoplastis* is corroborated by bands of similar size being conspicuously absent in the *V. ingenoplastis* lysate (Fig. 4*A*).

The apparent absence of proton pumping cI, cIII, and cIV in *V. ingenoplastis* implies that another mechanism is employed to maintain mitochondrial membrane potential in this flagellate. Plausibly, it can be maintained by utilizing ATP synthase to hydrolyze rather than synthesize ATP, pumping protons across the inner mitochondrial membrane, as described in the bloodstream form (BSF) of *T. brucei* (35, 36). The core ATP synthase is composed of a soluble F_1- and an insoluble membrane-bound F_o unit of multiple subunits each (37). It oligomerizes to facilitate the formation of cristae, the site of ATP synthesis by oxidative phosphorylation in typical aerobic

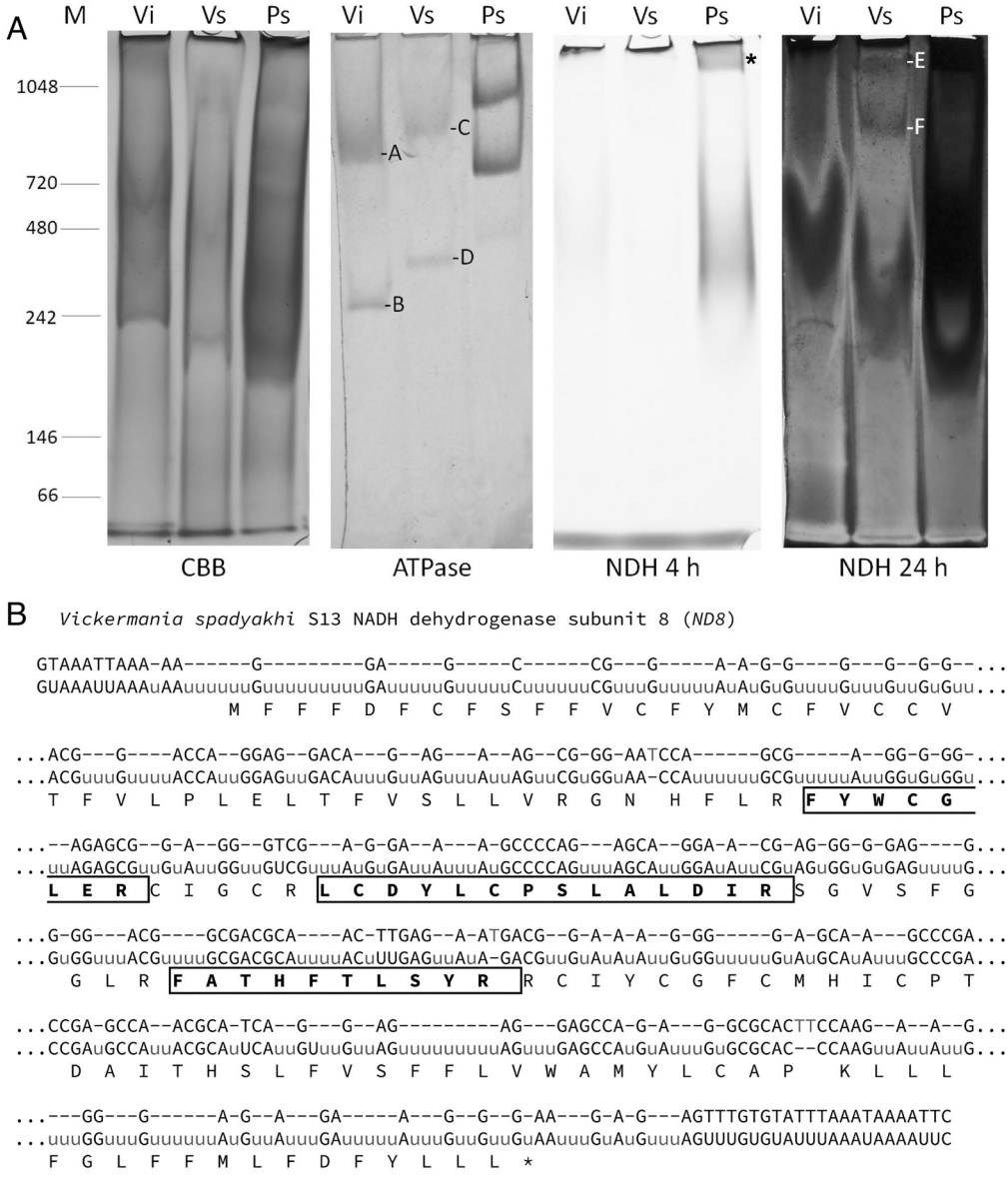

Fig. 4. Biochemical analyses of respiratory complexes I and V. (*A*) In-gel activity of *V. ingenoplastis* (Vi), *V. spadyakhi* (Vs), and *P. serpens* (Ps) mitochondrial lysates. Gels were stained with Coomassie brilliant blue in 2 to 10% native gel (panel CBB); complexes I and V were visualized by the in-gel staining of NADH dehydrogenase for 4 and 24 h (panels NDH), and ATP hydrolase activity for 4 h (panel ATPase). The asterisk indicates the position of complex I in *P. serpens*. Lower molecular weight smears in panels CBB and NDH 24 h resulted from the detergents used for membrane solubilization reacting with Coomassie brilliant blue or the phenazine methosulfate. Letters A-F indicate positions of bands analyzed by mass spectrometry. M is a protein molecular weight marker in kDa. (*B*) Mass spectrometry-identified peptides of *V. spadyakhi* ND8 (boxed).

eukaryotic cells, including trypanosomatids (38). To explore the role of this complex in the maintenance of mitochondrial membrane potential, we first confirmed its presence by an in-gel ATP hydrolysis activity assay utilizing the *Vickermania* species (Fig. 4*A*). The two bands observed in both *Vickermania* lanes presumably correspond to the F_1 subcomplex and the entire ATP synthase F_1F_o monomer (39). Mass spectrometry analysis of the excised F_1F_o band revealed an A6-derived peptide, consistent in sequence with its translated, reconstructed edited mRNA (*SI Appendix*, Fig. S5 and Dataset S3). A6 is part of the F_o unit.

Moreover, genes encoding all ATP synthase accessory proteins were detected in the nuclear genome of both *Vickermania* species with one notable exception—inhibitory factor 1 (IF1), a unidirectional inhibitor of ATP hydrolytic activity of the ATP synthase, which is widespread in eukaryotes, including trypanosomatids (40) (Dataset S2). The putative *IF1* gene in *V. spadyakhi* encodes a protein containing the entire N-terminal half shown to be sufficient for inhibition in *T. brucei* (41), but lacking a C-terminal region that is essential for the protein's homodimerization in numerous eukaryotes, including trypanosomatids (*SI Appendix*, Fig. S6). Thus, we expect that the truncated IF1 in *V. spadyakhi* is functional. Remarkably, the *IF1* homolog is apparently missing from the *V. ingenoplastis* genome. Its absence supports the attractive possibility that *V. ingenoplastis* ATP synthase operates in reverse to generate mitochondrial membrane potential.

Discussion

V. ingenoplastis was previously identified as a trypanosomatid with a morphologically unusual kDNA disk lacking typical minicircles (19, 27). We explored the evolution of molecular mechanisms and features of RNA editing and kDNA structure in both known *Vickermania* species, as our current knowledge of these traits is primarily dependent on that gleaned from the medically relevant representatives of the genera *Leishmania* and *Trypanosoma*.

The overall structure of the kDNA disk is remarkably conserved in trypanosomatids and does not change much even in *Blastocrithidia*, a group of trypanosomatid parasites with all three stop codons reassigned to encode amino acids (42). Thus, the unique drop-shaped structure of *Vickermania* kDNA may signal a profound deviation in its component molecules. Indeed, the size and motifs of its HL-circles depart substantially from the canonical kDNA minicircles of all other examined trypanosomatids, yet HL-circles still encode an extensive gRNA repertoire. We currently lack insight into the evolutionary (dis)advantages of large molecules with multiple gRNAs over minicircles containing one or few gRNA(s) that can be lost independently of one another. However, we hypothesize that the removal of nutrient restriction and other environmental stressors during growth in culture may be behind the shift for larger, less diverse, and less gRNA-populated HL-circles in *V. ingenoplastis* relative to those of *V. spadyakhi*. Nutrient-rich and stable culture conditions may allow a release from the selective pressure which drives two different phenomena. As observed in other species, such release could drive the loss of total HL-circle classes when their gRNAs direct an editing event that has become dispensable. However, it could also remove restrictions on molecule size. Energetically restrictive environments may disfavor the continued replication of increasingly larger molecules that are permissible under nutrient-rich culture conditions; in fact, gRNA-containing molecules in trypanosomatids tend to be relatively small.

Our characterization opens the door for experimentally addressing a range of questions in *Vickermania*: i) what is the functional role the HL-circle IRS sequences surrounding gRNA loci play in their transcription? Since gRNA-adjacent sequences in minicircles of other trypanosomatids are considered important for their expression (17), direct comparison of transcription between HL-circles and minicircles could shed light on the degree to which the process of gRNA expression is conserved; ii) how do links between gRNAs of the same or different transcripts influence changes to editing? iii) how does kDNA of *Vickermania* spp. replicate? The major differences between the *Vickermania* kDNA network and those of other trypanosomatids strongly indicate that the two mechanistically different forms of kDNA replication, well described in trypanosomatids examined thus far (1, 43), may not cover the whole spectrum of possibilities. In summary, such next steps will undoubtedly shed light onto the mechanisms of replication, maintenance, and processing of gRNA-encoding molecules in trypanosomatids.

Another distinguishing aspect of *Vickermania* biology is the presence of virtually acristate mitochondria (18). Cristae are the polymorphic invaginations of the inner membrane governing cellular respiration. In other organisms, including model trypanosomatids (44), the mitochondrial contact site and cristae organization system (MICOS) is considered the source of their biogenesis, while ATP synthase dimerization appears universally necessary to maintain the membrane shape (45). Moreover, the dissociation of ATP synthase dimers into monomers is tied to the loss of cristae (46). All the MICOS components (44) and subunits of ATP synthase implicated in dimerization (38) are present in both *Vickermania* spp. It is tempting to speculate that additional, yet-to-be-identified proteins fine-tune ATP synthase dimerization in these flagellates that, in turn, leads to an acristate phenotype. Additional work is needed to prove or disprove this hypothesis.

The two *Vickermania* spp. analyzed here significantly differ in several other aspects, most notably, in how they maintain mitochondrial membrane potential in the absence of cIII and cIV. *Vickermania spadyakhi* possesses a fully functional cI, which generates the membrane potential. Consequently, similarly to the majority of other trypanosomatids and aerobic eukaryotes (47), the organism uses ATP synthase in the canonical manner for ATP production. In contrast, the absence of cI in *V. ingenoplastis* implies other mechanisms for the membrane potential maintenance. The presence of complete ATP synthase strongly suggests that the parasite employs its reversed proton pumping activity to generate the membrane potential at the expense of ATP. This is reminiscent of the situation documented in the BSF of *T. brucei*, which also lacks proton pumping ETC complexes (35, 36). In the BSF, a strong downregulation of IF1 expression is critical to enable ATP synthase to switch into the reverse mode (40). In line with this, IF1 seems to have been lost in *V. ingenoplastis*, supporting the view of the obligatory reverse activity of ATP synthase. To the best of our knowledge, *V. ingenoplastis* would thus be the first known eukaryote that utilizes ATP synthase exclusively as an ATP-driven proton pump to maintain the membrane potential. Of note, functional elimination of cI through ablation of gRNAs mediating editing of its subunit cryptogenes in *V. ingenoplastis* is fascinating, but not unprecedented. A similar mechanism is apparently employed by the distantly related *L. tarentolae* and *Blastocrithidia nonstop* (16, 31).

In conclusion, exploration of the unique features of *Vickermania* provide insights not only into the relationship between gRNA complexity and kDNA structure but also into the variability and plasticity of this "evolutionary improbable" DNA structure, and other aspects of biology of these fascinating parasites.

Materials and Methods

Datasets Used. The sequencing datasets (total DNA and kDNA, total RNA, small RNA, and kRNA) and other technical details such as methods of library generation are listed in *SI Appendix*, Table S1 (BioProject PRJNA675748 for all

data, SRR31549343-SRR31549352). Previously released Illumina and Oxford Nanopore genomic data for *V. ingenoplastis* (24) were also used in the downstream analyses.

Additional methods for cultivation of trypanosomatids, isolation of nucleic acids, assembly and analysis of kDNA maxicircles and HL-circles, analysis of maxicircle transcripts and their editing, annotation of gRNAs, biochemical activity measurement of respiratory complexes and analysis of their nucleus-encoded subunits, proteomic analysis, and transmission electron microscopy can be found in *SI Appendix*.

Data, Materials, and Software Availability. All study data are included in the article and/or supporting information.

ACKNOWLEDGMENTS. We thank members of our laboratories for stimulating discussions and Martina Tesařová (Institute of Parasitology), Tereza Hromádková (University of Ostrava), and Daniel Monteyne (Université Libre de Bruxelles) for technical assistance. This work was primarily supported by the Czech Science Foundation (GAČR 22-01026S to J.L. and V.Y.). Additional support was provided by the European Union (EU)'s Operational Programme Just Transition (LERCO/22_003/0000003 to A.S. and V.Y.), the Czech Science Foundation (GAČR 23-07695S to A.B.), the Czech Ministry of Education, Youth and Sports (LUASK22033 to A.S. and V.Y., and /22_008/0004575 cofunded by the EU to O.G.), the Slovak Research and Development Agency (SK-CZ-RD-21-0038 to I.S.-S. and A.H.), the State assignment (121032300092-3 to E.G.), ACCORD project (ITMS2014+: 313021X329 to I.S.-S.), the Walloon Region, European Regional Development Fund, and the Fonds de la Recherche Scientifique Belgium (T.0178.21) to D.P.-M. The funders had no role in study design, data collection and analysis, decision to publish, or preparation of the manuscript.

Author affiliations: [a]Faculty of Biology, M.V. Lomonosov Moscow State University, Moscow 119991, Russia; [b]Life Science Research Centre, Faculty of Science, University of Ostrava, Ostrava 710 00, Czechia; [c]Department of Biochemistry, Faculty of Natural Sciences, Comenius University, Bratislava 842 15, Slovakia; [d]Institute of Parasitology, Biology Centre, Czech Academy of Sciences, České Budějovice 370 05, Czechia; [e]Faculty of Science, University of South Bohemia, 370 05 České Budějovice, Czechia; [f]Department of Glycobiology, Institute of Chemistry, Slovak Academy of Sciences, Bratislava 845 38, Slovakia; [g]Medirex Group Academy, Nitra 949 05, Slovakia; [h]de Duve Institute, Université Catholique de Louvain, Brussels 1200, Belgium; [i]Université Libre de Bruxelles, Gosselies 6041, Belgium; and [j]Department of Biomedical Sciences, University of Minnesota Medical School, Duluth, MN 55812

1. R. E. Jensen, P. T. Englund, Network news: The replication of kinetoplast DNA. *Annu. Rev. Microbiol.* **66**, 473–491 (2012).
2. I. Aphasizheva *et al.*, Lexis and grammar of mitochondrial RNA processing in trypanosomes. *Trends Parasitol.* **36**, 337–355 (2020).
3. K. Stuart, Trypanosomatids: Mitochondrial RNA editing. *Exp. Parasitol.* **68**, 486–490 (1989).
4. J. Lukeš, J. M. Archibald, P. J. Keeling, W. F. Doolittle, M. W. Gray, How a neutral evolutionary ratchet can build cellular complexity. *IUBMB Life* **63**, 528–537 (2011).
5. M. W. Gray, Evolutionary origin of RNA editing. *Biochemistry* **51**, 5235–5242 (2012).
6. J. Lukeš *et al.*, Trypanosomatids are much more than just trypanosomes: Clues from the expanded family tree. *Trends Parasitol.* **34**, 466–480 (2018).
7. V. David *et al.*, Gene loss and error-prone RNA editing in the mitochondrion of *Perkinsela*, an endosymbiotic kinetoplastid. *mBio* **6**, e01498-15 (2015).
8. A. Butenko *et al.*, Reductionist pathways for parasitism in euglenozoans? Expanded datasets provide new insights. *Trends Parasitol.* **37**, 100–116 (2021).
9. L. Simpson, The mitochondrial genome of kinetoplastid protozoa: Genomic organization, transcription, replication, and evolution. *Annu. Rev. Microbiol.* **41**, 363–382 (1987).
10. S. L. Zimmer, R. M. Simpson, L. K. Read, High throughput sequencing revolution reveals conserved fundamentals of U-indel editing. *Wiley Interdiscip. Rev. RNA* **9**, e1487 (2018).
11. B. L. Tylec *et al.*, Intrinsic and regulated properties of minimally edited trypanosome mRNAs. *Nucleic Acids Res.* **47**, 3640–3657 (2019).
12. E. S. Gerasimov *et al.*, Trypanosomatid mitochondrial RNA editing: Dramatically complex transcript repertoires revealed with a dedicated mapping tool. *Nucleic Acids Res.* **46**, 765–781 (2018).
13. R. M. Simpson, A. E. Bruno, J. E. Bard, M. J. Buck, L. K. Read, High-throughput sequencing of partially edited trypanosome mRNAs reveals barriers to editing progression and evidence for alternative editing. *RNA* **22**, 677–695 (2016).
14. J. Carnes *et al.*, *In vivo* cleavage specificity of *Trypanosoma brucei* editosome endonucleases. *Nucleic Acids Res.* **45**, 4667–4686 (2017).
15. D. A. Maslov *et al.*, Recent advances in trypanosomatid research: Genome organization, expression, metabolism, taxonomy and evolution. *Parasitology* **146**, 1–27 (2019).
16. D. A. Afonin *et al.*, *Blastocrithidia nonstop* mitochondrial genome and its expression are remarkably insulated from nuclear codon reassignment. *Nucleic Acids Res.* **52**, 3870–3885 (2024).
17. S. Cooper *et al.*, Assembly and annotation of the mitochondrial minicircle genome of a differentiation-competent strain of *Trypanosoma brucei*. *Nucleic Acids Res.* **47**, 11304–11325 (2019).
18. A. Kostygov *et al.*, *Vickermania* gen. nov., trypanosomatids that use two joined flagella to resist midgut peristaltic flow within the fly host. *BMC Biol.* **18**, 187 (2020).
19. S. Hajduk, "Studies of trypanosomatid flagellates with special reference to antigenic variation and kinetoplast DNA," Ph.D. thesis, Department of Zoology University of Glasgow, Glasgow, 1980), p. 229.
20. S. Aeschlimann, P. Stettler, A. Schneider, DNA segregation in mitochondria and beyond: Insights from the trypanosomal tripartite attachment complex. *Trends Biochem. Sci.* **48**, 1058–1070 (2023).
21. I. Kaurov *et al.*, The diverged trypanosome MICOS complex as a hub for mitochondrial cristae shaping and protein import. *Curr. Biol.* **28**, 3393–3407.e95 (2018).
22. F. G. Wallace, M. Wagner, W. E. Rogers, Varying kinetoplast ultrastructure in two subspecies of *Herpetomonas muscarum* (Leidy). *J. Protozool.* **20**, 218–222 (1973).
23. G. H. Coombs, "Herpetomonas muscarum ingenoplastis: An anaerobic kinetoplastid flagellate?" in *Biochemistry and Molecular Biology of "Anaerobic" Protozoa*, D. Lloyd, G. H. Coombs, T. A. Paget, Eds. (Harwood Academic Publishers, London, 1989), pp. 254–266.
24. C. M. d'Avila-Levy *et al.*, First draft genome of the trypanosomatid *Herpetomonas muscarum ingenoplastis* through MinION Oxford Nanopore technology and Illumina sequencing. *Trop. Med. Infect. Dis.* **5**, 25 (2020).
25. F. R. Opperdoes *et al.*, The remarkable metabolism of *Vickermania ingenoplastis*: Genomic predictions. *Pathogens* **10**, 68 (2021).
26. W. E. Rogers, F. G. Wallace, Two new subspecies of *Herpetomonas muscarum* (Leidy, 1856) Kent, 1880. *J. Protozool.* **18**, 645–654 (1971).
27. P. Borst, J. H. Hoeijmakers, S. Hajduk, Structure, function and evolution of kinetoplast DNA. *Parasitology* **82**, 81–93 (1981).
28. B. M. Porcel *et al.*, The streamlined genome of *Phytomonas* spp. relative to human pathogenic kinetoplastids reveals a parasite tailored for plants. *PLoS Genet.* **10**, e1004007 (2014).
29. E. S. Gerasimov *et al.*, Complete minicircle genome of *Leptomonas pyrrhocoris* reveals sources of its non-canonical mitochondrial RNA editing events. *Nucleic Acids Res.* **49**, 3354–3370 (2021).
30. D. S. Ray, Conserved sequence blocks in kinetoplast minicircles from diverse species of trypanosomes. *Mol. Cell Biol.* **9**, 1365–1367 (1989).
31. L. Simpson, S. M. Douglass, J. A. Lake, M. Pellegrini, F. Li, Comparison of the mitochondrial genomes and steady state transcriptomes of two strains of the trypanosomatid parasite, *Leishmania tarentolae*. *PLoS Negl. Trop. Dis.* **9**, e0003841 (2015).
32. E. S. Gerasimov *et al.*, Mitochondrial RNA editing in *Trypanoplasma borreli*: New tools, new revelations. *Comput. Struct. Biotechnol. J.* **20**, 6388–6402 (2022).
33. S. Cooper, E. S. Wadsworth, A. Schnaufer, N. J. Savill, Organization of minicircle cassettes and guide RNA genes in *Trypanosoma brucei*. *RNA* **28**, 972–992 (2022).
34. P. Čermáková, Z. Verner, P. Man, J. Lukeš, A. Horváth, Characterization of the NADH:Ubiquinone oxidoreductase (complex I) in the trypanosomatid *Phytomonas serpens* (Kinetoplastida). *FEBS J.* **274**, 3150–3158 (2007).
35. A. Schnaufer, G. D. Clark-Walker, A. G. Steinberg, K. Stuart, The F_1-ATP synthase complex in bloodstream stage trypanosomes has an unusual and essential function. *EMBO J.* **24**, 4029–4040 (2005).
36. S. V. Brown, P. Hosking, J. Li, N. Williams, ATP synthase is responsible for maintaining mitochondrial membrane potential in bloodstream form *Trypanosoma brucei*. *Eukaryot. Cell* **5**, 45–53 (2006).
37. A. Zíková, A. Schnaufer, R. A. Dalley, A. K. Panigrahi, K. D. Stuart, The F_0F_1-ATP synthase complex contains novel subunits and is essential for procyclic *Trypanosoma brucei*. *PLoS Pathog.* **5**, e1000436 (2009).
38. O. Gahura *et al.*, An ancestral interaction module promotes oligomerization in divergent mitochondrial ATP synthases. *Nat. Commun.* **13**, 5989 (2022).
39. C. Hierro-Yap *et al.*, Bioenergetic consequences of F_0F_1-ATP synthase/ATPase deficiency in two life cycle stages of *Trypanosoma brucei*. *J. Biol. Chem.* **296**, 100357 (2021).
40. B. Panicucci, O. Gahura, A. Zíková, *Trypanosoma brucei* TbIF1 inhibits the essential F_1-ATPase in the infectious form of the parasite. *PLoS Negl. Trop. Dis.* **11**, e0005552 (2017).
41. O. Gahura, B. Panicucci, H. Váchová, J. E. Walker, A. Zíková, Inhibition of F_1 -ATPase from *Trypanosoma brucei* by its regulatory protein inhibitor $TbIF_1$. *FEBS J.* **285**, 4413–4423 (2018).
42. A. Kachale *et al.*, Short tRNA anticodon stem and mutant eRF1 allow stop codon reassignment. *Nature* **613**, 751–758 (2023).
43. D. L. Guilbride, P. T. Englund, The replication mechanism of kinetoplast DNA networks in several trypanosomatid species. *J. Cell Sci.* **111**, 675–679 (1998).
44. L. R. Cadena, O. Gahura, B. Panicucci, A. Zíková, H. Hashimi, Mitochondrial contact site and cristae organization system and F1Fo-ATP synthase crosstalk is a fundamental property of mitochondrial cristae. *mSphere* **6**, e0032721 (2021).
45. W. Kuhlbrandt, Structure and mechanisms of F-Type ATP synthases. *Annu. Rev. Biochem.* **88**, 515–549 (2019).
46. K. M. Davies, C. Anselmi, I. Wittig, J. D. Faraldo-Gomez, W. Kuhlbrandt, Structure of the yeast F_1F_o-ATP synthase dimer and its role in shaping the mitochondrial cristae. *Proc. Natl. Acad. Sci. U.S.A.* **109**, 13602–13607 (2012).
47. F. R. Opperdoes, A. Butenko, P. Flegontov, V. Yurchenko, J. Lukeš, Comparative metabolism of free-living *Bodo saltans* and parasitic trypanosomatids. *J. Eukaryot. Microbiol.* **63**, 657–678 (2016).